出國報告（出國類別：國際研討會）

出席 2012 年「奈米孔洞及層狀材料在催化應用的挑戰」會議心得報告

服務機關：國防大學理工學院化學及材料工程學系
姓名職稱：文職教授　汪成斌
派赴國家：韓國
出國期間：101 年 8 月 3 日至 8 月 8 日
報告日期：101 年 8 月 16 日

摘要

2012 年「奈米孔洞及層狀材料在催化應用的挑戰」（Jeju Workshop）會議是由韓國西江大學主辦，大會地點為濟州華美達廣場酒店，為國際沸石小組重要的國際會議之一，因研討主題教侷限，參加人數以 100 人為上限，為一小型國際會議。參加人員來自世界各地，包括法國、愛爾蘭、捷克、澳大利亞、英國、西班牙、瑞士、南非、美國、韓國、日本、中國、台灣等多國之專家學者，此研討會投稿論文分口頭報告及壁報展示，共計 70 餘篇。在會議中聆聽各國學者之學術演講，其中以韓國學者 Sang-Eon Park 針對有機官能化的中孔矽材在異相催化的應用研究做一完整的回顧性報導;澳大利亞學者 Ajayan Vinu 探討中孔-巨孔分層排列的材料在感測器上的應用研究對我們現階段的研發受益最大。大會所討論之範圍包含新穎沸石材料的製備及應用、環境催化、能源、石化裂解之新穎材料等。世界各國學者齊聚一堂討論不同領域的研究成果與應用。本次會議提供個相當好的知識交流平台，藉由此學術交流進而瞭解國際未來研究發展方向及趨勢，真是獲益匪淺。此外，藉由參與大會各國專家學者之交換研究心得及吸取他人寶貴之研究經驗，將可做為本實驗室日後研究之參考。

筆者此次感謝獲國科會研究計畫之補助成行，發表題目共計二篇：“Catalytic Performance of Steam Reforming of Ethanol over SBA-15-Supported Cobalt Catalysts”，“Effect of Mg Modified on Co/SBA-15 Catalysts for Ethanol Steam Reforming”，達到與各國學者切磋交流的機會，並試乘了價值昂貴的氫能燃料電池汽車，真是獲益匪淺。

目次

頁碼

壹、 會議目的

2012 年「奈米孔洞及層狀材料在催化應用的挑戰」（Jeju Workshop）會議是由韓國西江大學主辦，為國際沸石小組每二年舉辦一次之國際學術會議。其會議宗旨在於結合世界各國有關新穎沸石材料的製備及應用之學者專家，就專長領域進行一系列學術研究成果發表及新知討論，以便交流最新進展和技術信息，歷年來所主辦之學術研究年會、研討會及專題討論會，皆對該學術領域有深遠的影響及貢獻。因此，藉由此學術交流進而瞭解國際未來研究發展方向及趨勢，並與各國專家學者交換研究心得及吸取他人寶貴研究經驗，將可做為日後研究之參考。

貳、 會議過程

(一)本會議屬於一小型國際研討會，參加人員約100員，分別來自世界各國之民間機構、專家學者及研究人員參與為期三天之學術論文發表討論會及旅遊。2012年「奈米孔洞及層狀材料在催化應用的挑戰」（Jeju Workshop）會議是由韓國西江大學主辦，於2012年8月3日至8月5日在濟州華美達廣場酒店舉行。此為沸石、奈米孔洞及層狀材料領域非常重要的研討會之一，與會者多為各國在該領域學有專精之教授與學者，本次台灣參與之人員僅三人(高雄大學及國防大學)。於此與各國學者相互交流之下獲益良多。

(二)本次研討會為一小型研討會，二天均安排於華美達廣場酒店中之大型演講廳及展示廳，分為邀請演講(INV)、口頭發表(OP)及壁報發表(PO)，其研究領域與大會流程如后。

Aug 3, 2012: 1. Emerging applications challenge zeolite synthesis (INV)

2. Extraframework In and Ga species in zeolites A, X and Y (INV)

3. Growth of uniformly oriented silica MFI and BEA zeolite films (INV)

4. New fundamental insights concerning formation de-Al 2-D zeolites (INV)

5. Quantum chemical investigation of layer zeolites (INV)

6. Flow synthesis of mesoporous silica catalysts for Knoevenagel condensation reaction (INV)
7. Organofunctionality of PMO for heterogeneous catalysis (INV)
8. Hierarchically ordered mesoporous materials on sensing application (INV)
9. Synthesis and adsorption/separation/catalytic applications of MIL-125 and NH_2-MIL-125 (INV)
10. Meso/microporous composite molecular sieves with coreshell structures: synthesis and applications (INV)

Aug 4, 2012: 1. MFI nanosheets with a mesopore-micropore hierarchy for catalysis (INV)
2. Targeted synthesis of porous frameworks with high surface area (INV)
3. Adsorption, storage and delivery of medically important gases (INV)
4. Catalytic performance of steam reforming of ethanol over SBA-15 supported cobalt catalysts (OP)
5. Catalytic pyrolysis of biomass component over mesoporous catalysts (OP)
6. Zeolite-beta supported Pt catalysts for hydrogenation/hydrodeoxygenation of pyrolysis oil model compounds (OP)
7. Facile preparation method for mesoporous MFI zeolite (OP)
8. Pure silica nanoparticles for liposome/lipase systemencapsulation (OP)
9. Storage of hydrogen in porous organic frameworks for clean energy applications (OP)
10. Surface and pore structure assessment of hierarchical MFI zeolites (OP)
11. Metal oxide nanosheets: synthesis and self-assembly into functional nanostructured materials (INV)
12. High selective adsorption in carbonized porous organic frameworks (INV)
13. Tubular silicalite-1 membrane for xylene separation (INV)
14. Transformation of aromatic hydrocarbons over zeolites (INV)

參、 會議心得

本研討會以沸石、奈米孔洞及層狀材料在催化應用的挑戰為主軸，會議是由韓國西江大學主辦，為該領域中相當重要之研討會。參加人員為世界各國之專家學者，此研討會投稿論文分口頭報告及壁報展示，共計70餘篇。大會所討論之範圍很廣，包含新穎沸石材料的製備及應用、環境催化、能源、石化裂解之新穎材料等。部份足以為我國所參考之依據，另相關論述主題亦十分具參考價值。

本人計有口頭報告及壁報展示各乙篇，透過各國學者不同領域的經驗，於問答間各取所需，達到智識精進功效，並積極與各國學者交換演講意見達到學術交流目的。經過此次研討會歷練，使本人對未來之研究更具信心，將持續於此領域探討研析，並且對於後續之研究將會秉持精益求精的精神戮力完成。本次會議提供個相當好的知識交流平台，藉由此學術交流進而瞭解國際未來研究發展方向及趨勢，真是獲益匪淺。

肆、 建議事項

本研討會為國際沸石小組重要的國際會議之一，因研討主題教侷限，參加人數的限制(以 100 人為上限)，為一小型國際會議，探討範圍以沸石、奈米孔洞及層狀材料之催化應用，值得相關研究人員與學者參與。建議未來可增加國內專家學者參與機會，藉以吸收國際新知並分享研究成果。很可惜，我的碩班研究生這次未獲得國科會的輔助，希望未來能在補助的員額及經費予以提高，鼓勵研究生積極參與國際會議，相信對國內各方面研究及學術工作的提昇，必定有所助益。願以此次的與會心得與大家分享共勉之，本次研討會攜回會議論文集資料。

作者發表之論文

Catalytic Performance of Steam Reforming of Ethanol over SBA-15 Supported Cobalt Catalysts

Catalytic Performance of Steam Reforming of Ethanol over SBA-15-Supported Cobalt Catalysts

Josh Y. Z. Chiou[1], Siao-Wun Liu[1], Wei-Ling Chang[1], Chin-Liang Lai[1], Chia-Chieh Shen[2,3,4] and Chen-Bin Wang[1*]

[1]Department of Chemical and Materials Engineering, Chung Cheng Institute of Technology, National Defense University, Tahsi, Taoyuan, Taiwan, ROC
[2]Fuel Cell Center, Yuan Ze University, Taoyuan 32003, Taiwan, ROC
[3]Department of Mechanical Engineering, Yuan Ze University, Taoyuan 32003, Taiwan, ROC
[4]Graduate School of Renewable Energy and Engineering, Yuan Ze University, Taoyuan 32003, Taiwan, ROC

Abstract

The Ca-modified cobalt catalysts supported on SBA-15 and Co/SiO_2 for hydrogen production by steam reforming of ethanol (SRE) has been studied to evaluate the catalytic activity, stability and the behavior of deposited carbon. The Ca/SBA-15 and Ca-SBA-15 supports are prepared from the $Ca(NO_3)_2 \cdot 4H_2O$ (10 wt%) which incorporates to SBA-15 by incipient wetness impregnation and direct hydrothermal methods. The active Co ($Co(NO_3)_2 \cdot 6H_2O$, Co content is 10wt%) is incorporated to SiO_2, SBA-15 and modified-SBA-15 supports with incipient wetness impregnation method to obtain the cobalt catalysts (assigned as Co/SiO_2, Co/SBA-15, Co-Ca/SBA-15 and Co/Ca-SBA-15, respectively). The catalytic activity of the SRE reaction is evaluated in a fixed-bed reactor. The results indicate that the Co/Ca-SBA-15 catalyst is preferential among these cobalt-based catalysts and the ethanol can be converted completely at 375 °C. The Y_{H2} approaches 4.76 at 500 °C and less coke deposition. Furthermore, the long-term stability test approaches 100 h at 500 °C and does not deactivate.

KEY WORDS: Cobalt catalysts; Ethanol; Steam reforming

*To whom the correspondence should be addressed.

E-mail address: chenbinwang@gmail.com and chenbin@ndu.edu.tw

1. Introduction

Nowadays, hydrogen becomes the most promising carbon free energy carrier for fuel cells, i.e. proton exchange membrane fuel cells (PEMFCs) that can provide clean and highly efficient electric power for both mobile and stationary applications [1]. It stores and delivers energy in a usable form, but it must be produced on-board from hydrocarbons or liquid fuels, i.e. alcohol like ethanol, has received much attention due to having several advantages when compared to hydrocarbons. From the environmental point of view the use of ethanol is preferred because renewable ethanol obtained from biomass offers high hydrogen content, non-toxicity, safe storage and easy handling [2-4]. Ethanol can be catalytically converted with active metals or metal oxides through steam reforming into a H_2-rich gas at a moderate temperature (range 300 ℃ to 600 ℃) [5-10]. Among these, Co-based catalysts exhibit appreciable activities for the C–C bond broken and water-gas shift (WGS) reaction. Supported cobalt catalysts showed a significant improvement of the catalytic performance, such as the low working temperature and low by-products generated are efficient in the SRE reaction. Haga et al. [11] found that the properties of the cobalt catalysts were greatly influenced by the supports. Among these catalysts, the Co/Al_2O_3 catalyst showed high hydrogen selectivity for SRE by suppressing the CO methanation and the ethanol decomposition. Llorca et al. [5] focused on the various oxides as supports that included acidic/basic and redox properties. In the designing of high efficiency SRE over Co/Al_2O_3 and Co/SiO_2 catalysts, Batista et al. [1] showed that the Co/SiO_2 catalyst possessed better CO removal capacity. Llorca et al. [12] reported that the prepared Co/ZnO catalyst from $Co_2(CO)_8$ precursor could obtain CO-free hydrogen and highly stable on the SRE reaction.

In order to improve the catalytic performance, doping extra components to modify the original properties is one method, the metals such as alkali (Li, Na and K) [13], alkaline earth (Mg and Ca) [14, 15] and lanthanide (La and Ce) [15] have been studied.

Pigos et al. [13] reported that the addition of Na and K over Pt/ZrO_2 catalyst significantly improved the formate decomposition rates on the WGS reaction. Wang et al. [14] reported that the addition of Na improved the catalytic performance of the $PtRu/ZrO_2$ catalyst for oxidative steam reforming of ethanol, where the added Na not only enhanced the WGS reaction at low temperature, but also depressed the coke deposition. Cheng et al. [15] suggested that the doped alkaline earth or lanthanide oxides in Ni/Al_2O_3 catalyst can promote the reforming CH_4 with CO_2 reaction.

Besides the above method, the choice of support with high surface area to disperse metal phase is the other way. The support materials such as ZSM-5 [16], MCM-41 [17] and SBA-15 [18] have been widely used in recently years, based on their large pores, thick walls and high thermal stability for high temperature catalytic reaction. Based on this regard, mesoporous material as support is considerable interest that gives an improvement on hydrogen production via steam reforming reaction [19-24]. Effect of alkaline earth metals (Mg and Ca) as promoter over Cu-Ni/SBA-15 [21] and $Cu-Ni/SiO_2$ [23] catalysts have been studied; both of them improved the dispersion of the metallic phase and metal-support interaction, where high hydrogen selectivity was obtained with Mg, while the incorporation of Ca depressed the coke deposition. Wang et al. [24] reported that pre-coating $Ce_xZr_{1-x}O_2$ layer on Ni-based SBA-15 catalyst can improve the redox property and enhance the catalytic activity on steam reforming of methane.

Co-based catalysts are well known to consider on the SRE reaction, while deactivation by the deposited carbon can not be avoided [25]. The SBA-15 supported Co-based catalysts with high surface area and modified by the Ca have been prepared in this work. This study aimed to develop a highly efficient and more stable Co-based catalyst for the SRE reaction to generate H_2 with high selectivity and low CO in the outlet gas. The catalytic performance and coking behavior via SRE over mesoporous structure catalysts are also considered.

2. Experimental

2.1 Catalyst Preparation

SBA-15 was prepared according to the method descrobed in the literature [18]. A triblock coplymer P123 (8 g, Strem) was dissolved in a solution of the 250 mL HCl (1.9 M).The solution was stirred at 40 ^{o}C for 2 h, and 16 g of tetraethyl orthosilicate (TEOS) was then solwly added to the mixture with vigorous stirring at 40 ^{o}C for 22 h. The solution was transferred into a Telfon bottle and aged at 100 ^{o}C for 24 h. The solid product was filtered, washed with deionized water and then dried at room temperature for 24 h, followed by calcination in air at 500 ^{o}C for 6 h.

The Ca/SBA-15 and Ca-SBA-15 supports were prepared from the $Ca(NO_3)_2 \cdot 4H_2O$ (10 wt%) which incorporated to SBA-15 by incipient wetness impregnation and direct hydrothermal methods. Obtained solid product was filtered, washed with deionized water and then dried at room temperature for 24 h, followed by calcination in air at 550 ^{o}C for 5 h. The active Co ($Co(NO_3)_2 \cdot 6H_2O$, Co content is 10wt%) is incorporated to SiO_2, SBA-15 and modified-SBA-15 supports with incipient wetness impregnation method and calcination in air at 400 ^{o}C for 3 h to obtain the cobalt catalysts (assigned as Co/SiO_2, Co/SBA-15, Co-Ca/SBA-15 and Co/Ca-SBA-15, respectively).

2.2 Catalyst Characterization

The metal loadings of catalysts were determined by the atomic-emission technique (ICP-AES) using a Perkin Elmer Optima 3000 DV instrument. The BET surface area and pore size distribution of the catalysts were measured by N_2 adsorption at liquid N_2 temperature using Micromeritics ASAP 2010 analyzer. X-ray diffraction (XRD) measurement was performed using a Siemens D5000 diffractometer with Cu $K_{\alpha 1}$ radiation (λ = 1.5406 Å) at 40 kV and 30 mA. The microstructure and particle size of the samples

were observed by using transmission electron microscopy (TEM) with a JEOL JEM-2010 microscope equipped with a field emission electron source and operated at 200 kV. The elemental analysis (EA) of the carbon was determined by a HERAEUS VarioEL-III analyzer. A thermogravimetry (TG) analysis was carried out using a Seiko SSC5000 TG system. The rate of heating was maintained at 10 ℃·min^{-1}. The measurement was carried out from RT to 1000 ℃ under an air flow rate of 100 mL·min^{-1}. Reduction behavior of the catalysts was studied by temperature programmed reduction (TPR). About 50 mg sample was heated in a flowing 10% H_2/N_2 gas (10 ml·min^{-1}) with a heating rate 7 ℃·min^{-1} from room temperature to 800 ℃. Hydrogen consumption was detected by a thermal conductivity detector (TCD).

2.3 Activity test

Catalytic activity of SBA-15-supported cobalt catalysts toward SRE reaction were performed at atmospheric pressure in a fixed-bed flow reactor. A catalyst amount of 100 mg was placed in a 4 mm i.d. quartz tubular reactor, held by glass-wool plugs. The temperature of the reactor was controlled by a heating tape, and measured by a thermocouple (1.2 mm i.d.) at the center of the reactor bed. The feed of the reactants was comprised of a gaseous mixture of ethanol (EtOH), H_2O and Ar (purity 99.9995%, supplied by a mass flow controller). The composition of the reactant mixture (H_2O/EtOH/Ar = 37/3/60 vol.%) was controlled by a flow Ar stream (22 ml·min^{-1}) through a saturator (maintained 120 °C) containing EtOH and H_2O. The gas hourly space velocity (GHSV) was maintained at 23,000 h^{-1} and H_2O/EtOH molar ratio was 13 (H_2O : EtOH = 80 : 20 by volume). Prior to the reaction, the sample was activated under air at 400 °C for 3 h. The SRE activity was tested stepwise, while increasing the temperature from 250 to 500 °C. The reaction products were separated with columns of Porapak Q (for CO_2, H_2O, C_2H_4, CH_3CHO, CH_3OCH_3 and EtOH) and Molecular Sieve 5Å (for H_2, CH_4 and CO) and

quantitatively analyzed by two sets of TCD-GC on line. Response factors for all products were obtained and the system was calibrated with appropriate standards before each catalytic test. The evaluation of SRE activity depended on the conversion of ethanol (X_{EtOH}), the distribution of products (mol %) and the yield of hydrogen (Y_{H2}, mol H_2/mol EtOH).

3. Results and discussion

3.1 Characterization of fresh catalyst

XRD patterns of the silica-supported cobalt catalysts are shown in Fig. 1. Small-angle XRD patterns [Fig. 1(A)] show that the main diffraction peaks assigned to (100), (110) and (200) reflections, respectively, which indicate that the ordered hexagonal mesostructure of SBA-15 and Ca-SBA-15 supported cobalt catalysts have been well retained. However, the mesostructure is destroyed on the Co-Ca/SBA-15 catalyst. High-angle XRD patterns [Fig. 1(B)] indicate that the main diffraction peaks of (220), (311), (511) and (440) are related to the cubic phase of Co_3O_4 (JCPDS No: 76-1802). However, no apparent diffraction peaks observed for the Co-Ca/SBA-15 sample, which maybe formed an amorphous $CoSiO_3$ spinel from the CoO and SiO_2. According to the (311) diffraction pattern of Co_3O_4 crystalline, the particle size can be calculated using the Scherrer equation [26]. The calculated average crystallite sizes are summarized in the 2nd column of Table 1. It can be found that Co_3O_4 peaks become wider for Co/SBA-15 and Co/Ca-SBA-15 samples. This indicates that the SAB-15 and direct synthesis of Ca-SBA-15 supported cobalt catalysts can be well dispersed and possess high surface area (list in the 3rd column of Table 1). As the mesoporous SBA-15 blocked and/or destroyed, the surface area decreased. Moreover, in Fig. 2, TEM images of these four catalysts are shown to reinforce these differences in terms of morphology and homogeneity of the active phase. The supported particles (dark zones) can be observed over the mesoporous

structure of SBA-15 and Ca-SBA-15 supports (long parallel channels in hexagonal array). This is in accordance with the small-angle XRD detection.

In order to further identify the cobalt species in these catalysts, the TPR is examined. Fig. 3 shows the TPR profiles of the silica-supported cobalt catalysts. According to previous reported [8], the Co_3O_4 could be subsequently reduced to CoO and Co. Three samples [Fig. 3(a) – (c)] possess two reduction peaks around 250 to 400 ^oC can be assigned as the consecutive reduction of Co_3O_4 to CoO and CoO to Co, respectively. The slight shift of reductive peaks to lower temperature for Co/Ca-SBA-15 sample [Fig. 3(c)] indicates that a well-dispersed of cobalt oxide may be possible. This is in accordance with the calculated average crystallite sizes from XRD detection. The TPR profile of Co-Ca/SBA-15 catalyst consists of low temperature peak around 318 °C [Fig. 3(d)] and high temperature peak around 800 °C. It demonstrates that minor cobaltic oxide and major $CoSiO_3$ spinel (which is difficult to be reduced) exist in this sample.

3.2 Catalytic performance

Fig. 4 summarizes the effect of temperature on X_{EtOH} of the silica-supported cobalt catalysts. Also, the catalytic performance of ethanol conversion, products distribution and hydrogen yield are summarized in 錯誤! 找不到參照來源。. The results confirm that the activity of Co/SiO_2, Co/SBa-15 and $Co/Ca\text{-}SiO_2$ catalysts are better than Co-Ca/SBA-15. According to the characterization, the destroyed of mesoporous structure of silica and formation of $CoSiO_3$ spinel for the Co-Ca/SBA-15 sample reduces the catalytic activity. The ethanol conversion approaches completion around 400 ℃ for the three samples while only 30% converts for the Co-Ca/SBA-15 sample. Although the activity at low temperature is preferential for the Co/SiO_2, the 100% conversion temperature (400 ℃) is higher than both the Co/SBA-15 and Co/Ca-SBA-15 samples (375 ℃). When comparing the effect of temperature on the decomposition of acetaldehyde (D_T), we see the easy

cracking of acetaldehyde promotes the increase of hydrogen yield (Y_{H2}). Nevertheless, the promoting effect of the mesoporous structure of silica is pronounced. The D_T of the Co/Ca-SBA-15 sample approaches 350 ℃ while it is above 375 ℃ for the Co/SiO_2 sample and exceeds 500 ℃ for the Co-Ca/SBA-15 sample. The Y_{H2} exceeds 4.0 around 400 ℃ and arrives 4.76 under 500 ℃ for the Co/Ca-SBA-15 sample, while, only 2.0 for the Co-Ca/SBA-15 sample at 500 ℃.

The pathway of the SRE reaction proposed in this work is described and shown in Scheme 1. The lower temperature (< 375 °C) presents large amounts of CH_3CHO and decreasing amounts of CH_3CHO with increase the temperature, that accompany the increasing H_2. Apparently, the dehydrogenation of ethanol to acetaldehyde is the first step. As the temperatures rise, the major reaction proceeds with acetaldehyde decomposition into methane and CO.

$$C_2H_5OH \rightarrow CH_3CHO + H_2 \quad (1)$$

$$CH_3CHO \rightarrow CH_4 + CO \quad (2)$$

In the presence of water, the side-reactions of water gas shift (WGS) reaction, steam reforming of methane, consecutive dehydrogenation from the methyl group and/or further react with surface OH groups or water may also occur.

$$CO + H_2O \rightarrow CO_2 + H_2 \quad (3)$$

$$CH_4 + H_2O \rightarrow CO + 3\,H_2 \quad (4)$$

Duo to the endothermic nature of steam reform of methane (ΔH_r = 206 kJ/mol), the reaction (7) is carried out at high temperatures (around 600 ~ 900 °C) to achieve high conversion rates [27-29]. From the minor distribution of CO and CH_4 for the silica-supported cobalt catalysts, pathway of (5) is impossible. Accompanied the WGS reaction with CO oxidation [30] derives the minor CO distribution. The methyl group can further react with surface OH species or water to form carbon monoxide and hydrogen [31] and/or consecutive dehydrogenation of methyl causes the coke formation.

Carbon deposition is considered to be the main cause for Co-based catalyst deactivation in steam reforming of ethanol [32]. The effect of support can be tuned with alkaline earth to obtain sufficient acid-base sites [33, 34] for water splitting into OH groups and limited acidic sites to avoid the formation of coke, which results from olefin polymerization. Fig. 5 compares the conversion and products distribution as a function of time-on-stream (TOS) during the SRE reaction over the Co/SBA-15 and Co/Ca-SBA-15 catalysts at 500 °C. The Co/SBA-15 catalyst retained complete conversion for around 8 h and the S_{H2} approached 70 %, while the S_{CO} was higher than 20% after 5 h. From the decrease of CO_2, the reverse water gas shift (RWGS) reaction may be occurred.

$$CO_2 + H_2 \rightarrow CO + H_2O \quad (5)$$

Modification of SBA-15 with Ca using direct hydrothermal can increase the basic sites that relieves the carbon deposition. The Co/Ca-SBA-15 catalyst displays the better durability. The activity maintains over 100 h and the S_{H2} also approaches 68 %, while the S_{CO} is higher than 10% after 50 h. The catalyst can maintain the long-term stability attributed to the deposited coke can be removed rapidly by the adsorbed hydroxyl on the calcium oxide to maintain the activity. The model of elimination of deposited coke on the Co/Ca-SBA-15 catalyst shows in the Scheme 2.

The TEM and EA qualitative and quantitative analysis can be used to characterize the deposited coke on the surface of catalyst. Fig 6 shows the TEM images for the Co/SBA-15 and Co/Ca-SBA-15 catalysts after the TOS test at 500 °C. Despite the higher stability of Co/Ca-SBA-15 catalyst, carbon deposition can not be completely suppressed; rather catalyst deactivation can only be slow down. The higher stability could be due to lower carbon deposition. Also, the EA analysis (list in the last two columns in Table 3) confirms that the deposited carbon is 5.7% (11 h TOS, rate is 0.52 $\%\cdot h^{-1}$) and 8.2% (100 h TOS, rate is 0.08 $\%\cdot h^{-1}$), respectively for the Co/SBA-15 and Co/Ca-SBA-15 catalysts. The images show that the deposited carbon appears as filaments and tubes emerged with the cobalt, or

as a rather coating carbon covered on the surface of catalyst. According to the deactivation with deposited carbon, the coating carbon would shorten the lifetime of catalyst rather than the filaments carbon [35], which convinced with our results. Moreover, the spent Co/Ca-SBA-15 catalyst with well thermal stability maintains the mesoporous structure and retards the growth of Co by sintering [Fig 6(B)] after the SRE reaction.

The results obtained for the ethanol conversion, CH_4 and CO composition, hydrogen yield and the amount of carbon on the silica-supported cobalt catalysts, which were determined from temperature-programmed experiments of the spent catalyst after the time-on-stream, are summarized in Table 3. The comparison of the performances of these catalysts showed that the support played the important role in the improvement of the catalytic performances in terms of stability in the presence of a deactivating impurity. The Co/Ca-SBA-15 catalyst displays the better catalytic activity and durability among these series cobalt-based catalysts.

Conclusions

The role of calcium can elevate the thermal stability and eliminate carbon deposited on cobalt catalyst. The role of SBA-15 can elevate the thermal stability and increase the dispersion of cobalt catalyst. Further, modification of SBA-15 with Ca using direct hydrothermal can increase the basic sites that relieves the carbon deposition. The Co/Ca-SBA-15 catalyst exhibits better catalytic activity and durability among the silica-supported cobalt catalysts. The Y_{H2} approaches 4.76 at 500 $^{\circ}$C and less coke deposition. Furthermore, the long-term stability test approaches 100 h at 500 $^{\circ}$C and does not deactivate. The deposited coke on the cobalt surface can be removed rapidly by the adsorbed hydroxyl on the calcium oxide to maintain activation.

Acknowledgement

We are pleased to acknowledge the financial support for this study by the National Science Council of the Republic of China under contract numbers of NSC 99-2113-M-606-001-MY3 and NSC 101-2623-E-155-001-ET.

References

[1] M.S. Batista, R.K.S. Santos, E.M. Assaf, J.M. Assaf, E.A. Ticianelli, J. Power Sources 134 (2004) 27-32.

[2] D.K. Liguras, D.I. Kondarides, X.E. Verykios, Appl. Catal. B43 (2003) 345-354.

[3] G. Maggio, S. Freni, S. Cavallaro, J. Power Sources 74 (2001) 17-23.

[4] L.F. Brown, Int. J. Hydrogen Energy 26 (2001) 381-397.

[5] J. Llorca, N. Homs, J. Sales, P. Ramirez de la Piscina, J. Catal. 209 (2002) 306-317.

[6] A. Haryanto, S. Fernando, N. Murali, S. Adhikari, Energy Fuels 19 (2005) 2098-2106.

[7] P.K. Cheekatamarla, C.M. Finnerty, J. Power Sources 160 (2006) 490-499.

[8] C.B. Wang, C.C. Lee, J.L. Bi, J.Y. Siang, J.Y. Liu, C.T. Yeh, Catal. Today 146 (2009) 76-81.

[9] J.Y. Siang, C.C. Lee, C.H. Wang, W.T. Wang, C.Y. Deng, C.T. Yeh, C.B. Wang, Int. J. Hydrogen Energy 35 (2010) 3456-3462.

[10] S.W. Liu, J.Y. Liu, Y.H. Liu, Y.H. Huang, C.T. Yeh, C.B. Wang, Catal. Today 164 (2011) 246-250.

[11] F. Haga, T. Nakajima, H. Miya, S. Mishima, Catal. Lett. 48 (1997) 223-227.

[12] J. Llorca, P. Ramirez de la Piscina, J.A. Dalmon, J. Sales, N. Homs, Appl. Catal. B43 (2003) 355-369.

[13] J.M. Pigos, C.J. Brooks, G. Jacobs, B.H. Davis, Appl. Catal. A. 328 (2007) 14-26.

[14] C.H. Wang, K.F. Ho, J.Y.Z. Chiou, C.L. Lee, S.Y. Yang, C.T. Yeh, C.B. Wang, Catal.

Commun. 12 (2011) 854-858.

[15] Z. Cheng, Q. Wu, J. Li, Q. Zhu, Catal. Today 30 (1996) 147-155.

[16] D.H. Olson, G.T. Kokotailo, S.L. Lawton, W.M. Meler, J. Phys. Chem. 85 (1981) 2238-2243.

[17] C.T. Kresge, M.E. Leonowicz, W.J. Roth, J.C. Vartuli, J.S. Beck, Nature 359 (1992) 710-712.

[18] D. Zhao, J. Feng, Q. Huo, N. Melosh, G.H. Fredrickson, B.F. Chmelka, G.D. Stucky, Science 279 (1998) 548-552.

[19] A.J. Vizcaíno, A. Carrero, J.A. Calles, Int. J. Hydrogen Energy 32 (2007) 1450-1461.

[20] A. Carrero, J.A. Calles, A.J. Vizcaíno, Appl. Catal. A 327 (2007) 82-94.

[21] A.J. Vizcaíno, A. Carrero, J.A. Calles, Catal. Today 146 (2009) 63-70.

[22] J.A. Calles, A. Carrero, A.J. Vizcaíno, Micropor. Mesopor. Mater. 119 (2009) 200-207.

[23] A. Carrero, J.A. Calles, A.J. Vizcaino, Chem. Eng. J. 163 (2010) 395-402.

[24] K. Wang, X. Li, S. Ji, X. Shi, J. Tang, Energy Fuels 23 (2009) 25-31.

[25] H. Wang, Y. Liu, L. Wang, Y. Qin, Chem. Eng. J. 145 (2008) 25-31.

[26] H.P. Klug, L.E. Alexander, X-ray Diffraction Procedures for Polycrystalline and Amorphous Materials, P. 491, Wiley, New York, 1962.

[27] M. Mamak, N. Coombs, G. Ozin, Adv. Mater. 12 (2000) 198-202.

[28] P. Bera, S. Mitra, S. Sampath, M.S. Hegde, Chem. Commun. (2001) 927-928.

[29] T. Takeguchi, S.N. Furukawa, M. Inoue, J. Catal. 202 (2001) 14-24.

[30] C.W. Tang, C.C. Kuo, M.C. Kuo, C.B. Wang, S.H. Chien, Appl. Catal. A309 (2006) 37-43.

[31] M. Domok, M. Toth, J. Rasko, A. Erdohelyi, Appl. Catal. B69 (2007) 262-272.

[32] H. Song, U.S. Ozkan, J. Catal. 261 (2009) 66-74.

[33] R.M. Navarro, M.A. Pena, J.L.G. Fierro, Chem. Rev. 107 (2007) 3952-3991.

[34] L.S. Carvalho, A.R. Martins, P. Reyes, A. Vicentini, M.C. Rangel, Catal. Today 142 (2009) 52-60.

[35] I. Suelves, M.J. Lázaro, R. Moliner, B.M. Corbella and J.M. Palacios, Int. J. Hydrogen Energy 30 (2005) 1555-1567.

Figure captions

1. XRD patterns of (A) Small angle (B) Wide angle of the silica-supported cobalt catalysts: (a) Co/SiO_2 (b) Co/SBA-15 (c) Co/Ca-SBA-15 (d) Co-Ca/SBA-15
2. TEM images of the silica-supported cobalt catalysts: (a) Co/SiO_2 (b) Co/SBA-15 (c) Co/Ca-SBA-15 (d) Co-Ca/SBA-15
3. TPR profiles of the silica-supported cobalt catalysts: (a) Co/SiO_2 (b) Co/SBA-15 (c) Co/Ca-SBA-15 (d) Co-Ca/SBA-15
4. Comparison of ethanol conversion over the silica-supported cobalt catalysts for the SRE reaction: (a) Co/SiO_2 (b) Co/Ca-SBA-15 (c) Co/SBA-15 (d) Co-Ca/SBA-15
5. Time-on-stream of SRE reaction at 500 °C: (A) Co/SBA-15 (B) Co/Ca-SBA-15
6. TEM images of spent catalysts: (A) Co/SBA-15 (B) Co/Ca-SBA-15

Table captions

1. Physical property of the silica-supported cobalt catalysts.
2. Steam reforming of ethanol over silica-supported cobalt catalysts.
3. Catalytic performance and carbon deposition on the silica-supported cobalt catalysts

Schemes

Scheme 1 Reaction pathway for the SRE reaction over silica-supported cobalt catalysts.

Scheme 2 Model of elimination of deposited coke on the Co/Ca-SBA-15 catalyst.

Table 1 Physical property of the supports and silica-supported cobalt catalysts

Sample	Co_3O_4 (311)* Particle size (nm)	Surface area (m^2/g)	Average Pore Size (nm)
SiO_2	—	506	2.1
Co/SiO_2	13.8	335	2.1
SBA-15	—	742	5.5
Co/SBA-15	11.4	348	3.8
Ca-SBA-15	—	688	4.9
Co/Ca-SBA-15	9.2	420	4.0
Ca/SBA-15	—	138	5.3
Co-Ca/SBA-15	—	92	3.5

*Debye-Scherrer equation.

Table 2 Steam reforming of ethanol over silica-supported cobalt catalysts

Catalyst	T_R (℃)	X_{EtOH} (%)	Y_{H2} (mol)	Products distribution (mol %)*						
				H_2	CH_4	CO	CO_2	C_2H_4	C_2H_4O	C_3H_6O
Co/SiO_2	250	24.2	0.60	46.5	—	—	—	—	53.5	—
	300	45.4	1.50	48.9	1.21	1.74	0.37	—	47.8	—
	350	79.5	2.29	55.5	1.90	5.96	1.43	0.73	32.6	1.96
	375	95.9	2.79	60.7	3.06	11.7	3.09	1.35	18.4	1.71
	400	100	3.45	66.9	6.61	7.18	19.2	—	—	0.10
	450	100	4.04	70.7	5.52	2.83	20.9	—	—	—
Co/SBA-15	300	2.78	1.52	49.4	—	—	—	6.70	43.9	—
	350	22.5	2.85	72.1	1.49	—	1.51	0.68	24.3	—
	375	100	3.02	69.5	10.5	6.71	6.05	0.04	7.10	—
	400	100	3.60	70.1	11.4	2.19	16.3	—	—	—
	450	100	4.02	70.2	12.1	0.54	17.2	—	—	—
	500	100	4.42	69.6	3.54	1.93	24.8	—	—	—
Co/Ca-SBA-15	250	2.75	0.08	33.8	—	—	—	—	66.3	—
	300	44.6	2.00	64.7	0.94	0.80	—	—	43.6	—
	350	80.5	2.27	63.7	1.10	3.34	1.43	—	30.4	—
	375	100	3.15	68.5	6.62	13.2	10.43	—	1.39	—
	400	100	4.15	71.0	4.20	4.58	20.2	—	—	—
	450	100	4.32	71.6	6.42	1.36	20.6	—	—	—
	500	100	4.76	71.5	2.91	1.64	23.9	—	—	—
Co-Ca/SBA-15	300	6.03	1.18	49.7	3.14	—	—	—	47.2	—
	350	12.3	1.32	51.4	4.95	—	1.38	—	42.3	—
	400	32.2	1.52	49.0	1.64	0.29	1.52	1.51	46.0	—
	450	50.3	1.87	48.9	1.06	0.50	1.67	1.78	46.1	—
	500	95.7	2.05	52.4	1.04	1.24	1.63	1.61	40.5	—

*Water not included.

Table 3 Catalytic performance and carbon deposition on the silica-supported cobalt catalysts

Catalyst	T_R (℃)	X_{EtOH} (%)	S_{CH4} (%)	S_{CO} (%)	Y_{H2} (mol)	TOS* (h)	Carbon deposition	
							EA (%)**	Rate (%/h)
Co/SiO_2	450	100	5.52	2.83	4.04	10	7.8	0.78
Co/SBA-15	500	100	3.54	1.93	4.42	11	5.7	0.52
Co/Ca-SBA-15	500	100	2.91	1.64	4.76	100	8.2	0.08
Co-Ca/SBA-15	500	95	1.04	1.24	2.05	—	—	—

* Time-on-stream of SRE reaction at 500 °C. **Measured by elemental analysis.

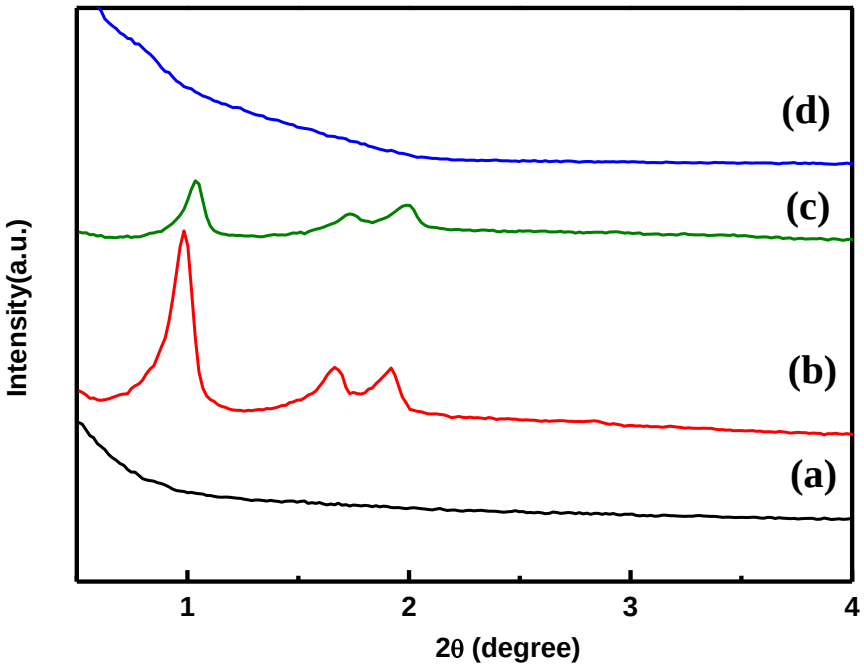
(d)
(c)
(b)
(a)
Intensity(a.u.)
1
2
3
4
2θ (degree)

Fig 1(A)

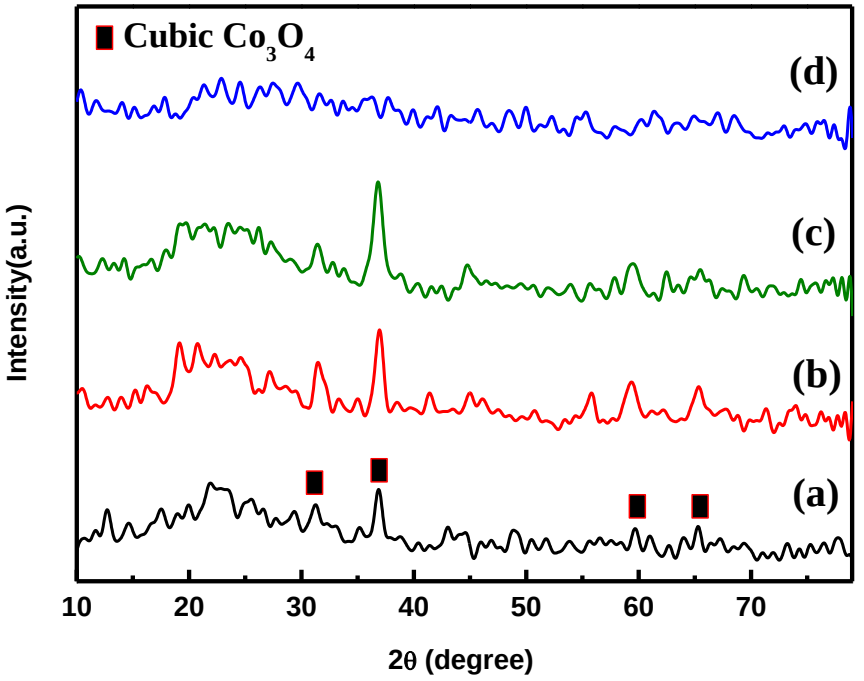
Cubic Co3O4
(d)
(c)
(b)
(a)
Intensity(a.u.)
10
20
30
40
50
60
70
2θ (degree)

Fig 1(B)

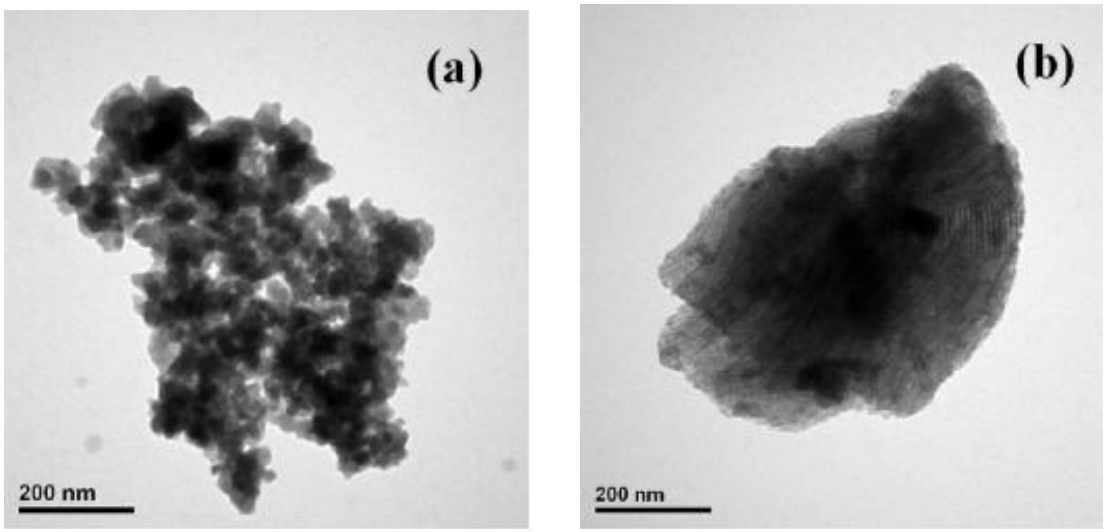

Fig 2

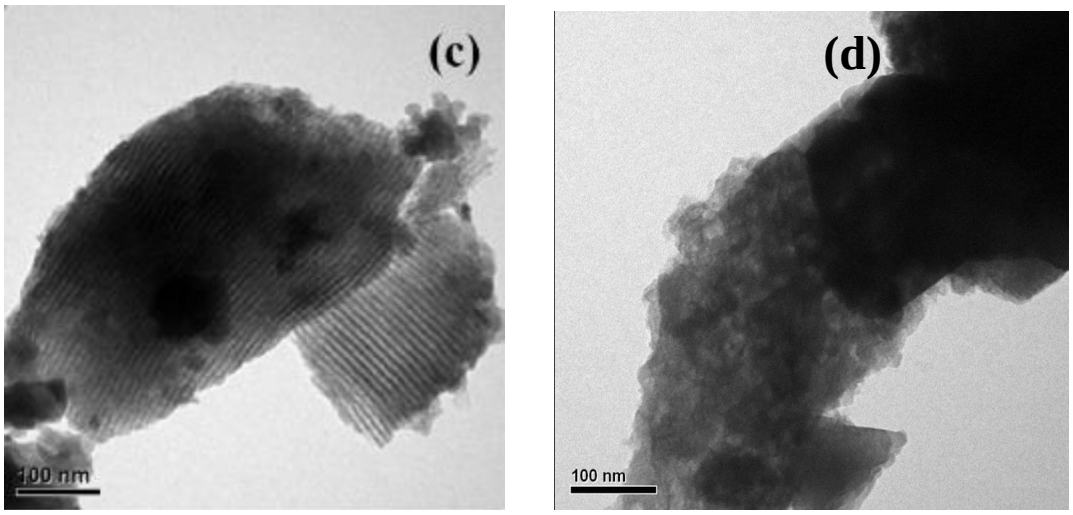

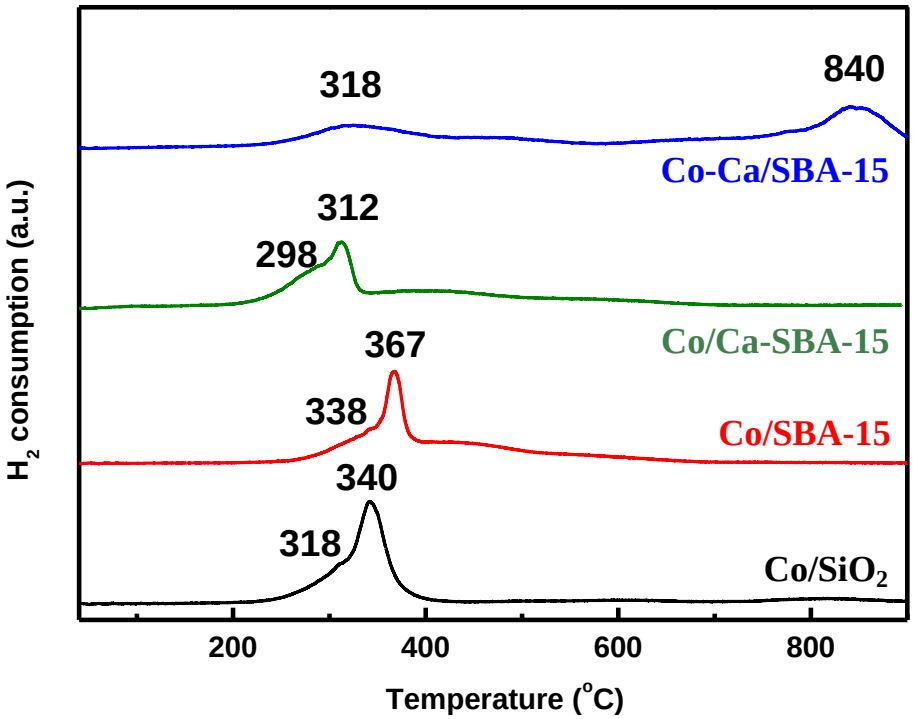
318
840
Co-Ca/SBA-15
312
298
Co/Ca-SBA-15
367
338
Co/SBA-15
340
318
Co/SiO2
H2 consumption (a.u.)
200
400
600
800
Temperature (°C)

Fig 3

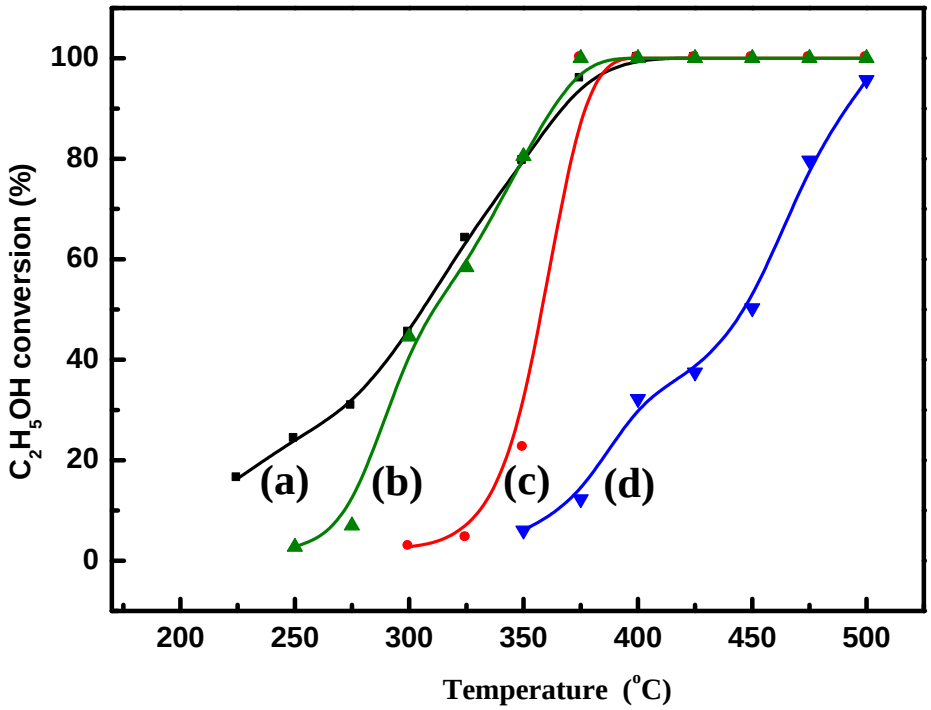
100
80
60
40
20
0
C2H5OH conversion (%)
(a)
(b)
(c)
(d)
200
250
300
350
400
450
500
Temperature (°C)

Fig 4

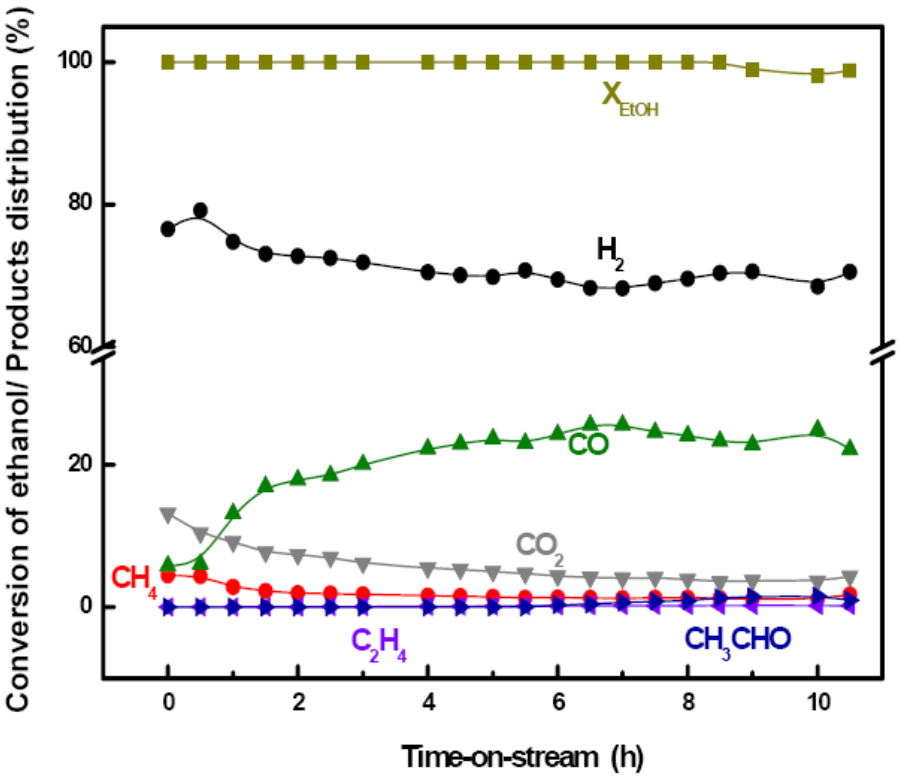
Conversion of ethanol/ Products distribution (%)
100
80
60
20
0
X_{EtOH}
H_2
CO
CO_2
CH_4
C_2H_4
CH_3CHO
0
2
4
6
8
10
Time-on-stream (h)

Fig 5(A)

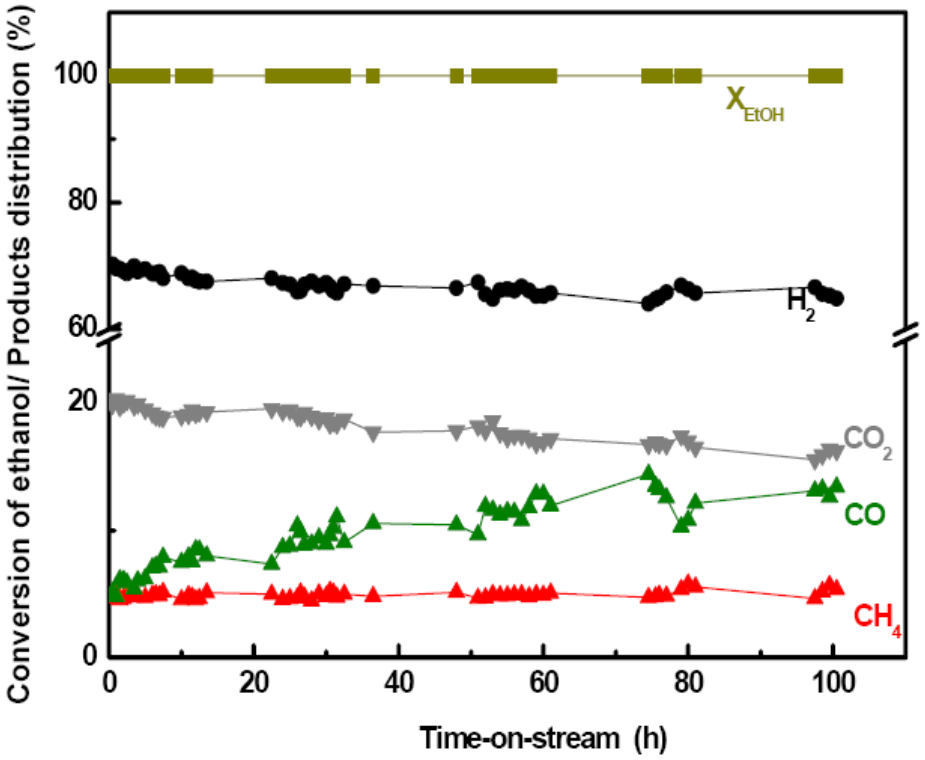
Conversion of ethanol/ Products distribution (%)
100
80
60
20
0
X_{EtOH}
H_2
CO_2
CO
CH_4
0
20
40
60
80
100
Time-on-stream (h)

Fig 5(B)

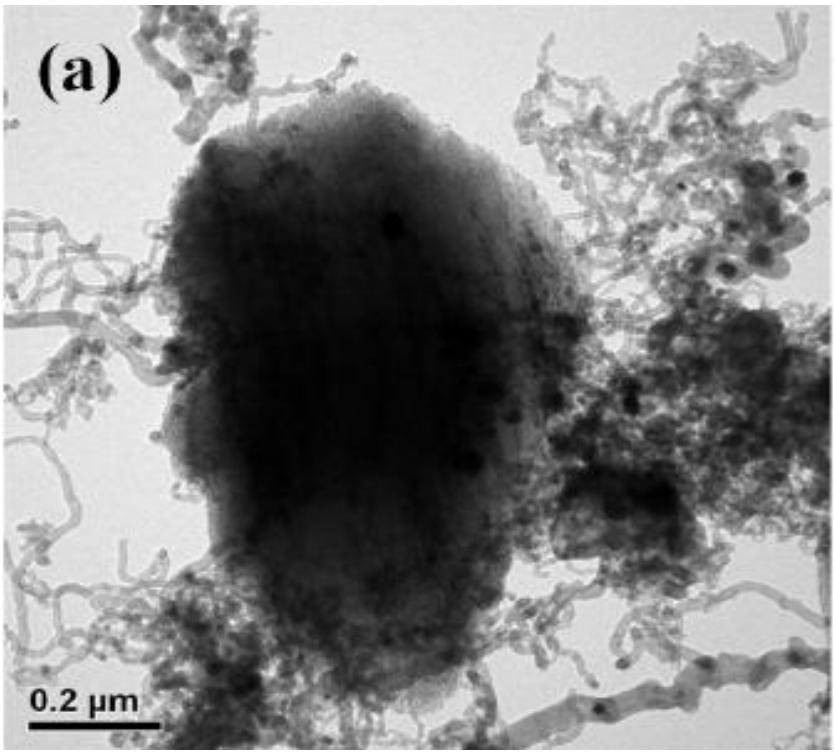

Fig 6(A)

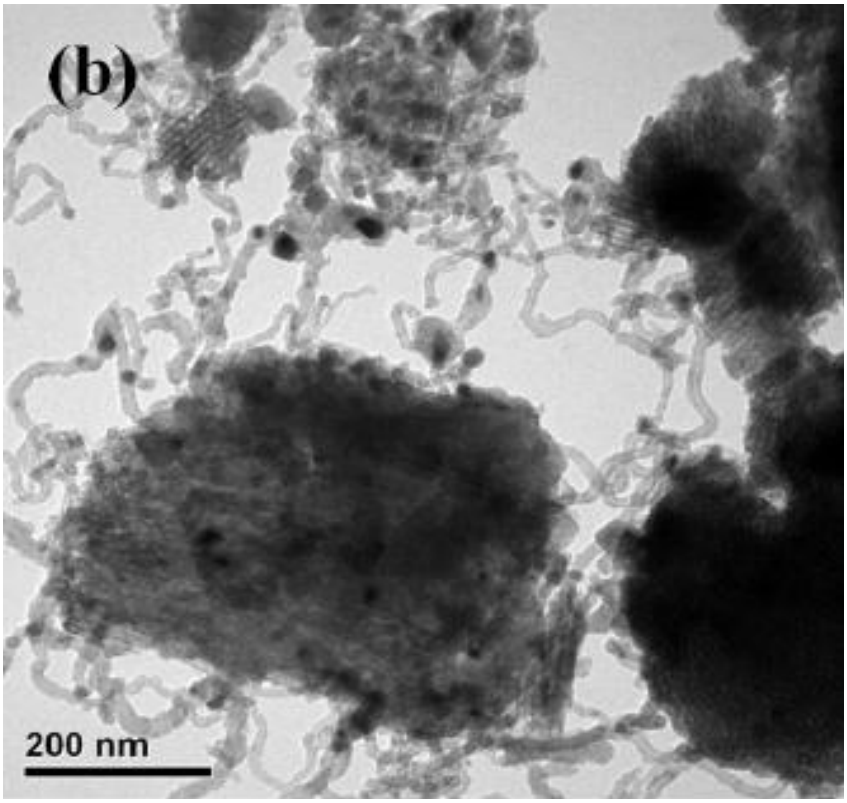

Fig 6(B)

Scheme 1

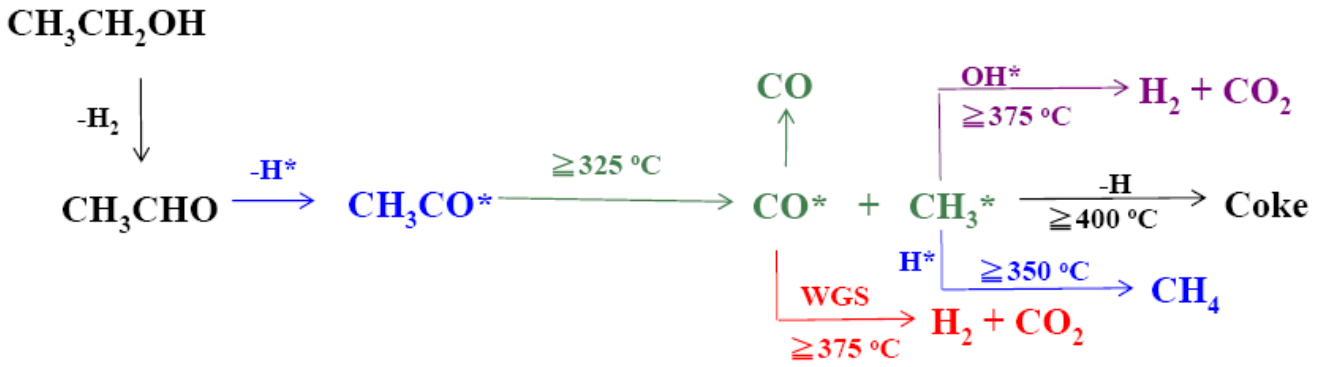

Scheme 2